Fermi National Accelerator Laboratory

FERMILAB-Pub-99/361-T

Single Top Quark Production at the LHC: Understanding Spin

Gregory Mahlon and Stephen Parke

Fermi National Accelerator Laboratory
P.O. Box 500, Batavia, Illinois 60510

January 2000

Submitted to *Physics Letters*

Operated by Universities Research Association Inc. under Contract No. DE-AC02-76CH03000 with the United States Department of Energy

Disclaimer

This report was prepared as an account of work sponsored by an agency of the United States Government. Neither the United States Government nor any agency thereof, nor any of their employees, makes any warranty, expressed or implied, or assumes any legal liability or responsibility for the accuracy, completeness, or usefulness of any information, apparatus, product, or process disclosed, or represents that its use would not infringe privately owned rights. Reference herein to any specific commercial product, process, or service by trade name, trademark, manufacturer, or otherwise, does not necessarily constitute or imply its endorsement, recommendation, or favoring by the United States Government or any agency thereof. The views and opinions of authors expressed herein do not necessarily state or reflect those of the United States Government or any agency thereof.

Distribution

Approved for public release; further dissemination unlimited.

Copyright Notification

This manuscript has been authored by Universities Research Association, Inc. under contract No. DE-AC02-76CH03000 with the U.S. Department of Energy. The United States Government and the publisher, by accepting the article for publication, acknowledges that the United States Government retains a nonexclusive, paid-up, irrevocable, worldwide license to publish or reproduce the published form of this manuscript, or allow others to do so, for United States Government Purposes.

Fermilab–Pub–99/361-T
McGill/99–39
SLAC-PUB-8317
hep-ph/9912458

arXiv:hep-ph/9912458 22 Dec 1999

Single Top Quark Production at the LHC: Understanding Spin

Gregory Mahlon*
Department of Physics, McGill University,
3600 University St., Montréal, Québec H3A 2T8, Canada

Stephen Parke†
Theoretical Physics Department
Fermi National Accelerator Laboratory
P.O. Box 500, Batavia, Illinois 60510, U.S.A.
and
Theory Group
Stanford Linear Accelerator Center
Stanford, California 94305, U.S.A.
(December 22, 1999)

Abstract

We show that the single top quarks produced in the Wg-fusion channel at a proton-proton collider at a center-of-mass energy $\sqrt{s} = 14$ TeV posses a high degree of polarization in terms of a spin basis which decomposes the top quark spin in its rest frame along the direction of the spectator jet. A second useful spin basis is the η-beamline basis, which decomposes the top quark spin along one of the two beam directions, depending on which hemisphere contains the spectator jet. We elucidate the interplay between the two- and three-body final states contributing to this production cross section in the context of determining the spin decomposition of the top quarks, and argue that the zero momentum frame helicity is undefined. We show that the usefulness of the spectator and η-beamline spin bases is not adversely affected by the cuts required to separate the Wg-fusion signal from the background.

14.65.Ha, 13.88.+e

Typeset using REVTEX

One of the many physics goals of the CERN Large Hadron Collider (LHC) program is a detailed study of the top quark. With a measured mass of 173.8 $\pm$ 5.2 GeV [1], the top quark is by far the heaviest known fermion, and the only known fermion with a mass at the electroweak symmetry-breaking scale. Thus, it is hoped that a detailed study of how the top quark couples to other particles will be of great utility in determining if the Standard Model mechanism for electroweak symmetry-breaking is the correct one, or if some type of new physics is responsible. Angular correlations among the decay products of polarized top quarks provide a useful handle on these couplings. One consequence of the large top quark mass is that the time scale for the top quark decay, set by its decay width Γ_t, is much shorter than the typical time required for QCD interactions to randomize its spin [2]: a top quark produced with spin up decays as a top quark with spin up. The Standard Model $V-A$ coupling of the W boson to the top quark leaves an imprint in the form of strong angular correlations among the decay products of the top quark [3].

The purpose of this letter is to demonstrate that single top quark production in the Wg fusion channel at LHC energies provides a copious source of polarized top quarks. Although possessing a larger production cross section, top quark *pairs* at the LHC do not dominantly populate a single spin configuration in any basis, because the initial state is primarily gg [4]. On the other hand, the Wg fusion channel is the largest source of single top quarks at the LHC. At the most basic level, Wg fusion is an electroweak process, with the produced top quarks coupled directly to a W boson. Therefore, it is not surprising to learn that these top quarks are strongly polarized. However, as has been shown in studies for other colliders [4–7], the appropriate spin basis for the top quark is not the traditional helicity basis. The essential point is that unless the particle whose spin is being studied is produced in the ultrarelativistic regime, there is no reason to believe that the helicity basis will provide the simplest description of the physics involved. Top quarks produced in pp collisions via Wg fusion at a center of mass energy $\sqrt{s} = 14$ TeV typically posses a speed of only $\beta \sim 0.6$ in the zero momentum frame (ZMF). Furthermore, the helicity of a massive particle is frame-dependent: the direction of motion of the top quark changes as we boost from frame to frame. This is significant, since, as we shall show, it is not possible to unambiguously define the ZMF. Thus, although we can pin down the ZMF well enough to say that the typical speed of the top quarks is $\beta \sim 0.6$ in that frame, we cannot do so with the precision required to compute the top quark spin decomposition in the ZMF helicity basis. Instead, we are left with the options of measuring the top quark helicity in the laboratory frame (LAB helicity basis), or using some other basis. Fortunately, it is simple to construct a spin basis in which well over 90% of the top quarks are produced in one of the two possible spin states.

We begin by outlining the computation of the single top quark production cross section, which is shown schematically in Fig. 1. The calculation which we will use for our spin analysis may be described as "leading order plus resummed large logs." For simplicity, we do not include the additional tree-level $2 \to 3$ and one-loop $2 \to 2$ diagrams which would be required for a full next-to-leading order computation. The neglected contributions turn out to be numerically small (about 2.5% of the total) at LHC energies [8].

Early calculations of the Wg fusion process were based solely on the $2 \to 3$ diagrams of Fig. 1c [9–15]. These diagrams are dominated by the configuration where the final state $\bar{b}$ quark is nearly collinear with the incoming gluon. In fact, they become singular as the mass of the b quark is taken to zero. This mass singularity appears as the large logarithm

$\ln(m_t^2/m_b^2)$.[1] Furthermore, at each order in the strong coupling, there are logarithmically enhanced contributions, converting the perturbation expansion from a series in α_s to one in $\alpha_s \ln(m_t^2/m_b^2)$. To deal with this situation, a formalism which sums these collinear logarithms to all orders by introducing a b quark parton distribution function has been developed [16–18] and subsequently applied to Wg fusion [8,19–21]. The large logarithms which caused the original perturbation expansion to converge slowly are resummed to all orders and absorbed into the b quark distribution, which turns out to be perturbatively calculable. Once the b quark distribution has been introduced, we must reorder perturbation theory, and begin with the $2 \to 2$ process shown in Fig. 1a. The $2 \to 3$ process then becomes a correction to the $2 \to 2$ contribution. However, because the logarithmically enhanced terms within the $2 \to 3$ contribution have been summed into the b quark distribution, there is overlap between the $2 \to 2$ and $2 \to 3$ processes: simply summing their contributions will result in overcounting. To account for this, we should subtract that portion of the $2 \to 3$ diagram where the gluon splits into a (nearly) collinear $b\bar{b}$ pair. Schematically, we indicate this by the diagram in Fig. 1b. Equivalently, we should subtract the first term from the series of collinear logarithms which were summed to produce the b quark distribution. This point of view is reflected by the prescription for computing Fig. 1b: we simply use the $2 \to 2$ amplitude, but we replace the b quark parton distribution function with the (lowest-order) probability for a gluon to split into a $b\bar{b}$ pair:

$$b_0(x,\mu^2) = \frac{\alpha_s(\mu^2)}{2\pi} \ln\left(\frac{\mu^2}{m_b^2}\right) \int_x^1 \frac{dz}{z} P_{qg}(z) g\left(\frac{x}{z},\mu^2\right). \tag{1}$$

Eq. (1) contains the DGLAP splitting function

$$P_{qg}(z) = \tfrac{1}{2}[z^2 + (1-z)^2]. \tag{2}$$

The total single top quark production cross section then consists of the $2 \to 2$ process minus the overlap plus the $2 \to 3$ process. As is emphasized in Ref. [18], the division among the three kinds of contributions is arbitrary and depends upon our choice of the QCD factorization scale. Different choices in factorization scale correspond to a reshuffling of the contributions among the three terms.

The production cross sections for single t and $\bar{t}$ quarks will be unequal at the LHC. An initial state u, $\bar{d}$, $\bar{s}$, or c quark is required for t production, whereas $\bar{t}$ production requires an initial state $\bar{u}$, d, s or $\bar{c}$ quark. Since the LHC is a pp collider, we expect more t quarks than $\bar{t}$ quarks, since the protons contain more valence u quarks than d quarks. This expectation is met by the total cross sections we obtain: 159 pb for t production and 96 pb for $\bar{t}$ production.[2] Table I summarizes the contributions from each flavor of light quark in the initial state. We see that for t production, the initial state contains an up-type quark 80%

[1] More precisely, this logarithm reads $\ln[(Q^2+m_t^2)/m_b^2]$ where Q^2 is the virtuality of the W boson.

[2] All of the cross sections reported in this paper were computed using the CTEQ5HQ parton distribution functions [22], two-loop running α_s, and the factorization scales advocated in Ref. [8].

of the time, while for $\bar{t}$ production, the initial state contains a down-type quark 69% of the time. In the following discussion, we will talk in terms of the dominant initial states, although when presenting the final spin beakdowns, all flavors will be included.

We are now ready to discuss the spin of the top quarks produced at LHC energies, beginning with the $2 \to 2$ contributions. For a final state t, the dominant $2 \to 2$ process is $ub \to dt$. In the ZMF of the initial state partons, the outgoing t and d quarks are back-to-back. Now the initial state contains a massless u quark and an effectively massless b quark. Since they couple to a W boson, we know they have left-handed chirality. Since they are both ultrarelativistic fermions, this left-handed chirality translates into left-handed helicity. Thus, the initial spin projection is zero. The final state d quark is also massless, and so its left-handed chirality also implies left-handed helicity. Conservation of angular momentum then leads to the t quark having left-handed helicity *in this frame*. Since the t quark is massive, boosting to another frame will, in general, introduce a right-handed helicity component. In particular, if we measure the helicity of the top quark in the laboratory frame instead of the ZMF, we find that it is left-handed only 66% of the time.

Turning to the $2 \to 3$ process, we find that the addition of a third particle to the final state frees the top quark from its obligation to have left-handed helicity in the ZMF. In fact, we find that left-handed tops are produced only 82% of the time by this process. Again, this number changes if we boost out of the ZMF: the fraction of left-handed helicity tops is only 59% in the lab frame.

When we come to the overlap contribution, we discover that it is not possible to unambiguously define the ZMF. Should we define the ZMF in terms of the light quark and gluon, or in terms of the light quark and the b quark which descended from the gluon via splitting? These two frames are different, and, as we have already argued, the helicity of the top quark is not invariant under the longitudinal boosts connecting these two frames.

Another way of illustrating the difficulty is to consider the question of experimentally reconstructing the ZMF. To determine the ZMF, we would have to account for *all* of the final state particles. With real detectors, this is clearly impossible, since particles with small transverse momenta or very large pseudorapidity tend to be missed. But the $2 \to 3$ process frequently contains a low-p_T $\bar{b}$ quark, which is likely to escape detection. Even with a perfect detector, it is still not possible to decide whether a given event came from the $2 \to 2$ diagram of Fig. 1a or the $2 \to 3$ diagram of Fig. 1c. The point is, a perfect detector would also track the proton remnants as well as the actual scattering products. Since there is no intrinsic bottom in the proton, after a $2 \to 2$ interaction there would be a $\bar{b}$ quark among the proton remnants hitting our "perfect" detector. As far as the detector is concerned, such a $\bar{b}$ quark would look identical to the $\bar{b}$ quark generated by the $2 \to 3$ process. The best that could be done is to observe that a $\bar{b}$ quark associated with the proton remnant would tend to have a much smaller p_T than one associated with the $2 \to 3$ diagram. However, the kinematics of the two processes overlap, rendering the location of the dividing line arbitrary. This is precisely the physics of the statement made earlier that the division of contributions among the $2 \to 2$, $2 \to 3$, and overlap terms is arbitrary, and depends on the QCD factorization scale [18].

Rather than use the (undefined) ZMF helicity basis, we should decompose the top quark spin in a manner which does not depend on any particular frame. The spectator basis, introduced in Ref. [7], provides such a means. This basis is based upon the observation

that when we decompose the top quark spin along the direction of the d-type quark, the spin down contribution is small. The $2 \to 2$ process produces no spin down t quarks in this basis, which is equivalent to measuring the helicity of the t quark in the frame where the t quark and d-type quark are back-to-back. The overlap contribution, being just the $2 \to 2$ process computed with Eq. (1) in place of the b quark distribution function, shares a common spin structure with the $2 \to 2$ process in this basis. The amplitude for spin-down t quark production via the $2 \to 3$ diagrams is suppressed by its lack of a singularity when the b quark mass is taken to zero [7]. Since the d-type quark appears in the spectator jet 80% of the time, if we simply use the direction of the spectator jet as the top quark spin axis, we obtain a high degree of polarization: 92% of the top quarks associated with the $2 \to 3$ process are produced with spin up in this basis. Combining the three contributions, we find that over-all fraction of spin up quarks in the spectator basis is 95%.

For $\bar{t}$ production the situation is a bit different. The d-type quark is in the final state only 31% of the time; in the remainder of the events, it is supplied by one of the beams. Hence, the spectator basis chooses the "wrong" direction for the spin axis the majority of the time! However, the spectator jet is simply the scattered light quark. In the Wg fusion process, the momentum transfer via the t-channel W boson deflects the incoming light quark just a little. Thus, the spectator jet momentum points in nearly the same direction as the original light quark momentum. This fact is reflected in the large (absolute) values of pseudorapidity at which the spectator jet usually emerges. Since the spectator jet and initial light quark posses nearly parallel momentum vectors, it does not degrade the degree of spin polarization very much to use the spectator jet direction even when the d-type quark was actually in the initial state. Overall, we find that 93% of the $\bar{t}$'s are produced with spin down in the spectator basis, which is only slightly worse than the situation for t's.

Since the d-type quark really comes from one of the two beams the majority of the time, it is worthwhile to consider the beamline basis in addition to the spectator basis. From Ref. [4] we recall that the beamline basis is defined by decomposing the $\bar{t}$ spin along the direction of one of the beams as seen in the $\bar{t}$ rest frame. Hence, there are two different beamline bases, since the two beams are not back-to-back in the $\bar{t}$ rest frame. We want to choose the beam which supplied the light quark. As we noted in the previous paragraph, the spectator jet typically points in the same direction as the beam which supplied the light quark. Therefore, we should choose to decompose the $\bar{t}$ spin along the beam which is most-nearly aligned with the spectator jet on an event-by-event basis. That is, we define the η-beamline basis as follows: if the pseudorapidity of the spectator jet is positive, choose the right-moving beam as the spin axis. If the pseudorapidity of the spectator jet is negative, choose the left-moving beam as the spin axis. In terms of the η-beamline basis we find that 90% of the $\bar{t}$'s have spin down. While this is somewhat worse than simply using the spectator basis, matters may be improved by using only those events where the spectator jet has a pseudorapidity which is larger in magnitude than some cut value η_{min}. This takes advantage of the fact that an initial state d quark is a valence quark. Thus, on average, it carries a bigger longitudinal momentum fraction than a quark plucked from the sea. As a result, the spectator jet from such events tends to be produced at (slightly) larger pseudorapidity than events initiated by $\bar{u}$, s, or $\bar{c}$ quarks. So a minimum pseudorapidity requirement increases the chances that the chosen beam actually does contain the d-type quark. For example, choosing $\eta_{min} = 2.5$ results in a spin decomposition very similar to that obtained in the spectator basis. Because

such a cut on the spectator jet pseudorapidity is envisioned by the experiments in order to separate the signal from the background [23], there is no disadvantage to including a minimum $|\eta|$ requirement in our definition of the η-beamline basis.

For convenience, we have summarized our results for the spin decompositions of single t and $\bar{t}$ production at the LHC in Tables II and III. The final column of both tables contains the spin asymmetry $(N_\uparrow - N_\downarrow)/(N_\uparrow + N_\downarrow)$. This is the quantity which appears in the differential distribution of the decay angle [3]:

$$\frac{1}{\sigma_T}\frac{d\sigma}{d\cos\theta} = \frac{1}{2}\left[1 + \frac{N_\uparrow - N_\downarrow}{N_\uparrow + N_\downarrow}\cos\theta\right]. \tag{3}$$

In Eq. (3), θ is the angle between the charged lepton (from the decaying top quark) and the chosen spin axis, as measured in the top quark rest frame.[3] Obviously, we want to make the spin asymmetry as large as possible in order to make this angular correlation easier to observe. From Tables II and III we see that the spectator basis produces correlations which are about a factor of 3 larger than in the LAB helicity basis. The improvement provided by the η-beamline basis is comparable.

Figs. 2 and 3 present the p_T distributions of the produced t and $\bar{t}$ quarks. In addition to the total cross section, we have plotted the contributions from the dominant spin component in the LAB helicity, spectator, and η-beamline bases.

In general, the spin of the top quark depends upon the point in phase space at which it is produced. Therefore, it is important to make an assessment of the impact of the experimental cuts which are imposed to isolate the signal from the background. Although a full-scale detector simulation is beyond the scope of this letter, we have investigated the effect of the following theorists' cuts:

$$\begin{array}{ll}
\text{missing energy:} & \not{p}_T > 15 \ \text{GeV}, \\
\text{lepton:} & p_T > 15 \ \text{GeV}, \ |\eta| < 2.5 \\
\text{spectator jet:} & p_T > 50 \ \text{GeV}, \ 2.5 < |\eta| < 5.0 \\
\text{bottom jet:} & p_T > 50 \ \text{GeV}, \ |\eta| < 2.5 \\
\text{isolation cut:} & \sqrt{(\Delta\eta)^2 + (\Delta\varphi)^2} > 0.4, \ \text{all pairs} \\
\text{third jet:} & \text{none with } p_T > 30 \ \text{GeV}, \ |\eta| < 2.5.
\end{array} \tag{4}$$

These cuts are similar to the ones used in the ATLAS design study [23]. Because these cuts tend to bias towards events where the top quark has a large velocity in the ZMF (to the extent that the ZMF can be defined), we expect that the spin fractions will be higher in their presence. Indeed this is the case, as may be seen from Tables IV and V. Even in the presence of cuts, both the spectator and η-beamline bases outperform the LAB helicity basis

[3]To describe the decay of a $\bar{t}$ quark, we should replace $\cos\theta$ by $-\cos\theta$ in Eq. (3). Since the $\bar{t}$'s are primarily spin down in the bases we are considering, the $\bar{t}$ spin asymmetry will be negative. Thus, the t and $\bar{t}$ samples may be combined without diluting the resulting angular correlations in the event that the sign of the charged lepton cannot be determined.

by more than a factor of 2 with regard to the magnitude of the angular correlations present in the final state. For t events, the spectator basis is slightly better than the η-beamline basis. For $\bar{t}$ events, the η-beamline basis is slightly better than the spectator basis. In both cases, however, the differences are so small that it would certainly be worthwhile to do the experimental analysis using both bases, especially since some of the systematics will differ in the two cases.

To summarize, we have seen that it is not possible to uniquely define the zero momentum frame of the initial state partons in the Wg-fusion process at the LHC. Consequently, when studying the spin of the produced top quarks, it does not make sense to use the ZMF helicity basis. Instead, we must use a spin basis whose definition does not depend on the existence of a well-defined ZMF. Simply using the LAB helicity basis results in a description of the top quarks where both spin components are comparable in size. However, there are spin bases where the top quarks are described primarily by just one of the two possible spin states. Two such bases are the spectator and η-beamline bases. In the spectator basis, we decompose the spin of the top quark in its rest frame along the direction of the spectator jet as seen in that frame. In the η-beamline basis we decompose the spin of the top quark in its rest frame along the direction of one of the proton beams as seen in that frame. The right-moving beam is chosen if the pseudorapidity of the spectator jet is positive, whereas the left-moving beam is chosen if the pseudorapidity of the spectator jet is negative. We find that both of these bases the spin angular correlations are approximately a factor of 3 larger than in the LAB helicity basis. The utility of these two bases is not adversely affected by the imposition of the sorts of cuts required to extract a Wg fusion signal from the background.

ACKNOWLEDGMENTS

We would like to thank Dugan O'Neil for prompting us to think carefully about the relationship between the $2 \to 2$ and $2 \to 3$ processes. We would also like to thank Scott Willenbrock and Zack Sullivan for their helpful discussions concerning their calculation [8] of the next-to-leading order Wg-fusion cross section. SJP would like to thank the SLAC theory group for their support and hospitality during the initial stages of this work.

The Fermi National Accelerator Laboratory is operated by Universities Research Association, Inc., under contract DE-AC02-76CHO3000 with the U.S.A. Department of Energy. High energy physics research at McGill University is supported in part by the Natural Sciences and Engineering Research Council of Canada and the Fonds pour la Formation de Chercheurs et l'Aide à la Recherche of Québec. SLAC is supported by the U.S.A. Department of Energy under contract DE-AC03-76SF00515.

REFERENCES

* Electronic address: mahlon@physics.mcgill.ca
† Electronic address: parke@fnal.gov

[1] C. Caso, *et al,* Eur. Phys. J. **C3** (1998) 1, and 1999 off-year partial update for the 2000 edition available on the PDG WWW pages (URL: `http://pdg.lbl.gov/`).
[2] I. Bigi, Y. Dokshitzer, V. Khoze, J. Kühn, and P. Zerwas, Phys. Lett. **181B**, 157 (1986).
[3] M. Jeżabek and J.H. Kühn, Phys. Lett. **B329**, 317 (1994). [hep-ph/9403366]
[4] G. Mahlon and S. Parke, Phys. Rev. **D53**, 4886 (1996). [hep-ph/9512264]
[5] S. Parke and Y. Shadmi, Phys. Lett. **B387**, 199 (1996). [hep-ph/9606419]
[6] G. Mahlon and S. Parke, Phys. Lett. **B411**, 173 (1997). [hep-ph/9706304]
[7] G. Mahlon and S. Parke, Phys. Rev. **D55**, 7249 (1997). [hep-ph/9611367]
[8] T. Stelzer, Z. Sullivan, and S. Willenbrock, Phys. Rev. **D56**, 5919 (1997). [hep-ph/9705398]
[9] S. Dawson, Nucl. Phys. **B249**, 42 (1985).
[10] S. Willenbrock and D.A. Dicus, Phys. Rev. **D34**, 155 (1986).
[11] S. Dawson and S. Willenbrock, Nucl. Phys. **B284**, 449 (1987).
[12] C.–P. Yuan, Phys. Rev. **D41**, 42 (1990).
[13] R.K. Ellis and S. Parke, Phys. Rev. **D46**, 3785 (1992).
[14] G.V. Jikia, and S.R. Slabospitsky, Sov. J. Nucl. Phys. **55**, 1387 (1992); Phys. Lett. **B295**, 136 (1992); Yad. Fiz. **55**, 2491 (1992) [Phys. At. Nucl. **55**, 1387 (1992)].
[15] D.O. Carlson, and C.P. Yuan, Phys. Lett. **B306**, 386 (1993).
[16] F. Olness and W.–K. Tung, Nucl. Phys. **B308**, 813 (1988).
[17] R. Barrett, H. Haber, and D. Soper, Nucl. Phys. **B306**, 697 (1988).
[18] M. Aivazis, J. Collins, F. Olness, and W.–K. Tung, Phys. Rev. **D50**, 3102 (1994). [hep-ph/9312319]
[19] F. Anselmo, B. van Eijk, and G. Bordes, Phys. Rev. **D45**, 2312 (1992).
[20] G. Bordes and B. van Eijk, Z. Phys. **C57**, 81 (1993).
[21] G. Bordes and B. van Eijk, Nucl. Phys. **B435**, 23 (1995).
[22] H.L. Lai, J. Huston, S. Kuhlmann, J. Morfin, F. Olness, J. Owens, J. Pumplin, and W.K. Tung, "Global QCD Analysis of Parton Structure of the Nucleon: CTEQ5 Parton Distributions," hep-ph/9903282.
[23] ATLAS Collaboration, "ATLAS Detector and Physics Performance," vol. 2, Report No. CERN-LHCC-99-15 (ATLAS-TDR-15), 1999 (unpublished).

FIGURES

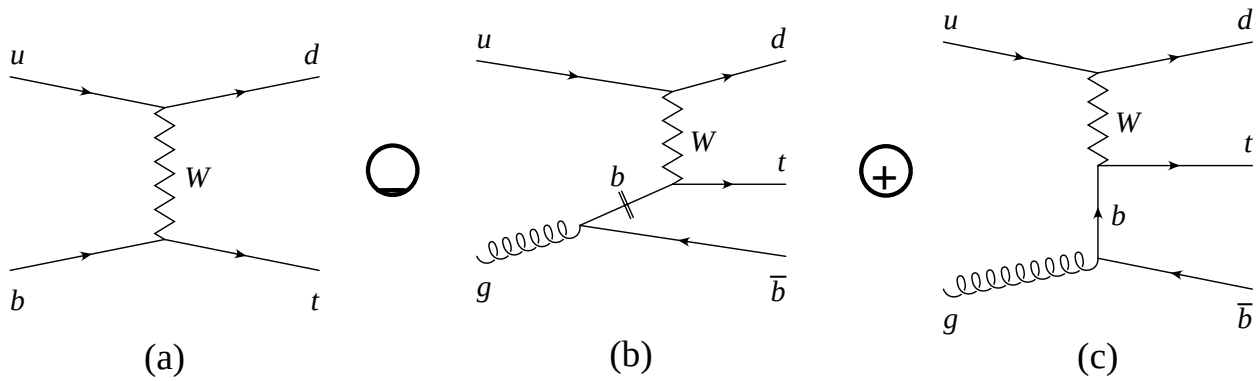

FIG. 1. Representative Feynman diagrams for single top quark production via Wg fusion.

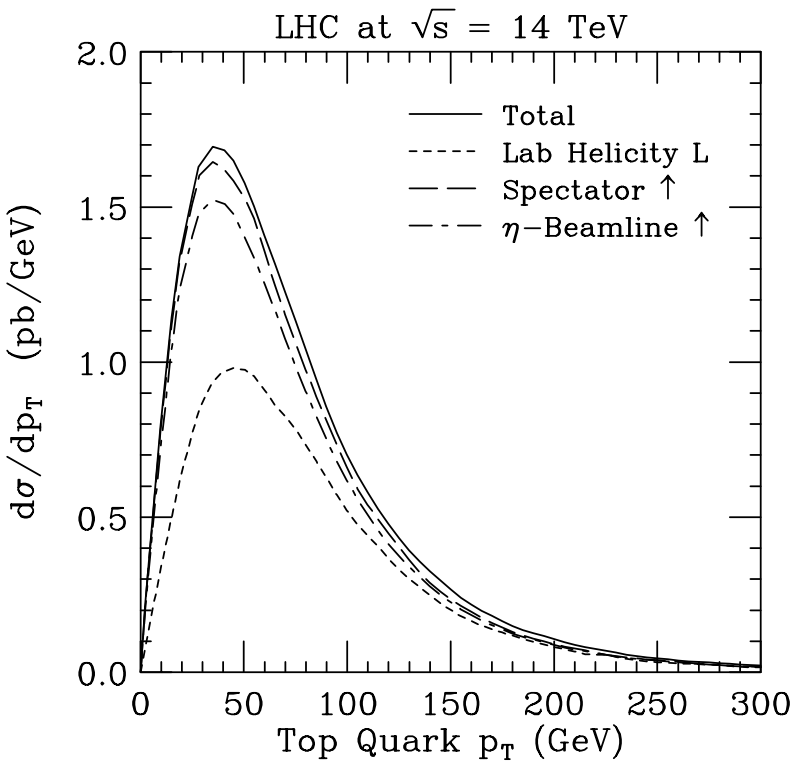

FIG. 2. The differential cross sections (total, LAB helicity basis left, spectator basis up, and η-beamline basis up (with $\eta_{min} = 0$)) as a function of the top quark transverse momentum for single top quark production via Wg fusion at the LHC with a center of mass energy of 14 TeV.

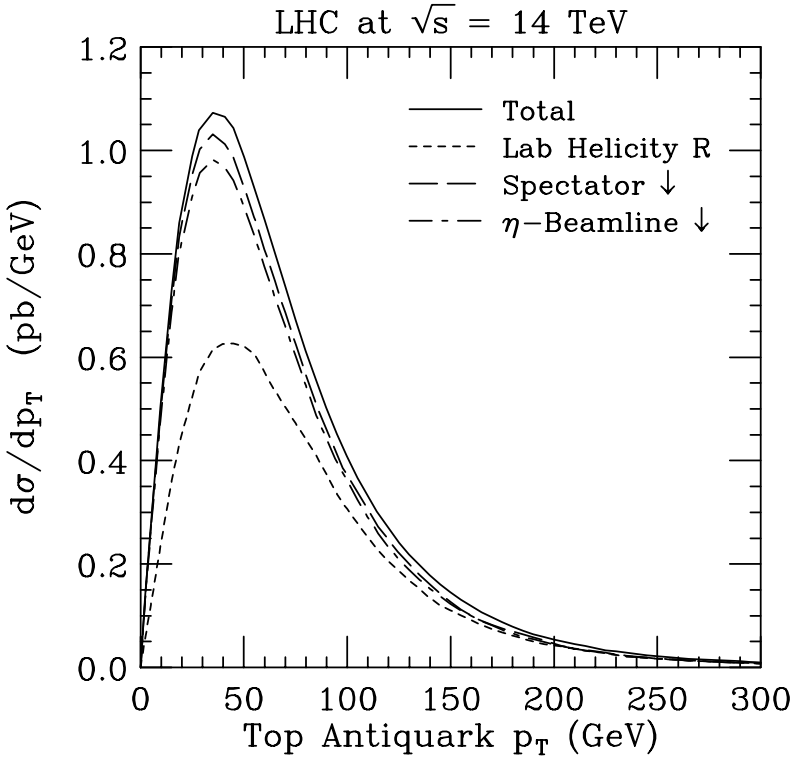

FIG. 3. The differential cross sections (total, LAB helicity basis right, spectator basis down, and η-beamline basis down (with $\eta_{min} = 0$)) as a function of the top antiquark transverse momentum for single top antiquark production via Wg fusion at the LHC with a center of mass energy of 14 TeV.

TABLES

TABLE I. Fractional cross sections for single top and single antitop production in the Wg fusion channel at the LHC at 14.0 TeV, decomposed according to the flavor of the light quark appearing in the initial state.

q	t	$\bar{t}$
u	74%	20%
d	12%	56%
s	8%	13%
c	6%	11%

TABLE II. Dominant spin fractions and asymmetries for the various bases studied for single top quark production in the Wg fusion channel at the LHC at 14.0 TeV. In addition to the total spin fractions, we have listed the fractions associated with each of the three types of diagrams (Figs. 1a–c) contributing to the total.

basis	$2 \to 2$	overlap	$2 \to 3$	total	$\frac{N_\uparrow - N_\downarrow}{N_\uparrow + N_\downarrow}$
LAB helicity	66% $\downarrow$(L)	64% $\downarrow$(L)	59% $\downarrow$(L)	64% $\downarrow$(L)	-0.27
ZMF helicity	99% $\downarrow$(L)	undefined	82% $\downarrow$(L)	undefined	undefined
spectator	99% $\uparrow$	99% $\uparrow$	92% $\uparrow$	95% $\uparrow$	0.89
η-bml, $\eta_{min} = 0$	93% $\uparrow$	93% $\uparrow$	86% $\uparrow$	88% $\uparrow$	0.77
η-bml, $\eta_{min} = 2.5$	97% $\uparrow$	97% $\uparrow$	90% $\uparrow$	93% $\uparrow$	0.85

TABLE III. Dominant spin fractions and asymmetries for the various bases studied for single top antiquark production in the Wg fusion channel at the LHC at 14.0 TeV. In addition to the total spin fractions, we have listed the fractions associated with each of the three types of diagrams (Figs. 1a–c) contributing to the total.

basis	$2 \to 2$	overlap	$2 \to 3$	total	$\frac{N_\uparrow - N_\downarrow}{N_\uparrow + N_\downarrow}$
LAB helicity	67% $\uparrow$(R)	64% $\uparrow$(R)	60% $\uparrow$(R)	65% $\uparrow$(R)	0.29
ZMF helicity	97% $\uparrow$(R)	undefined	78% $\uparrow$(R)	undefined	undefined
spectator	98% $\downarrow$	97% $\downarrow$	91% $\downarrow$	93% $\downarrow$	-0.87
η-bml, $\eta_{min} = 0$	94% $\downarrow$	94% $\downarrow$	88% $\downarrow$	90% $\downarrow$	-0.79
η-bml, $\eta_{min} = 2.5$	99% $\downarrow$	99% $\downarrow$	91% $\downarrow$	94% $\downarrow$	-0.87

TABLE IV. Dominant spin fractions and asymmetries for the various bases studied for single top quark production in the Wg fusion channel at the LHC at 14.0 TeV, subject to the set of cuts described in Eq. (4). In addition to the total spin fractions, we have listed the fractions associated with each of the three types of diagrams (Figs. 1a–c) contributing to the total.

basis	$2 \to 2$	overlap	$2 \to 3$	total	$\frac{N_\uparrow - N_\downarrow}{N_\uparrow + N_\downarrow}$
LAB helicity	75% $\downarrow$(L)	74% $\downarrow$(L)	71% $\downarrow$(L)	74% $\downarrow$(L)	−0.48
spectator	100% $\uparrow$	100% $\uparrow$	99% $\uparrow$	99% $\uparrow$	0.99
η-bml	99% $\uparrow$	99% $\uparrow$	98% $\uparrow$	98% $\uparrow$	0.96

TABLE V. Dominant spin fractions and asymmetries for the various bases studied for single top antiquark production in the Wg fusion channel at the LHC at 14.0 TeV, subject to the set of cuts described in Eq. (4). In addition to the total spin fractions, we have listed the fractions associated with each of the three types of diagrams (Figs. 1a–c) contributing to the total.

basis	$2 \to 2$	overlap	$2 \to 3$	total	$\frac{N_\uparrow - N_\downarrow}{N_\uparrow + N_\downarrow}$
LAB helicity	72% $\uparrow$(R)	70% $\uparrow$(R)	67% $\uparrow$(R)	70% $\uparrow$(R)	0.41
spectator	99% $\downarrow$	99% $\downarrow$	97% $\downarrow$	98% $\downarrow$	−0.96
η-bml	100% $\downarrow$	100% $\downarrow$	98% $\downarrow$	99% $\downarrow$	−0.97